Reverse Electron Transfer in Ru/HfB_2 Drives Selective Hydrogenation via Strong Metal–Support Coupling

Xianlang Chen,[a] *Chengkang Zhou,*[a] *Guoquan Zhou,*[d] *Saisai Wang,*[b] *Songpei Zhang,*[b] *Tongyang Song,*[a] *Rongrong Li,*[a,*] *Haiting Cai,*[b,*] *Bolin Wang,*[c] *Yuxue Yue,*[b,*] *Jia Zhao*[b]

[a] Engineering Research Center of Recycling & Comprehensive Utilization of Pharmaceutical and Chemical Waste of Zhejiang Province, Taizhou University, Taizhou 318000, Zhejiang, China.

[b] Industrial Catalysis Institute of Zhejiang University of Technology, Hangzhou 310014, Zhejiang, China.

[c] School of Chemical Engineering, Northeast Electric Power University, 132012, Jilin, China.

[d] Zhejiang Institute of Tianjin university， Ningbo City, Zhejiang Province 315211, P. R. China.

Rongrong Li - Email: lrr@tzc.edu.cn

Haiting Cai - Email: caihaiting@zjut.edu.cn

Yuxue Yue - Email: yueyuxue@zjut.edu.cn

* Corresponding Author

Materials and Catalysts Preparation

All chemicals were obtained from commercial sources and used without further purification. Hafnium powder (Alfa-Aesar, >99.6% purity) and amorphous boron (Aldrich, 95-97% purity) were employed as starting materials, with an excess of boron added to compensate for potential loss during synthesis. In a typical procedure, 200 mg of HfB_2 was ultrasonically dispersed in deionized water, followed by the addition of 2.05 mL of $RuCl_3$ aqueous solution (0.005 g/mL). The mixture was stirred for four hours to ensure uniform dispersion. Subsequently, 10 mL of freshly prepared $NaBH_4$ aqueous solution (4 mg/mL) was introduced, and the mixture was stirred for an additional hour. The resulting solution was filtered, and the residue was thoroughly washed with deionized water. The collected solid was dried overnight in an oven, ground into a fine powder, and designated as Ru/HfB_2 (2.5 wt.% Ru). For comparative analysis, a reference Ru/C catalyst was prepared using the same protocol. This method ensures consistent synthesis conditions, enabling a direct comparison of the catalytic performance between Ru/HfB_2 and Ru/C.

Catalysts Evaluation

In this study, all catalytic reactions were carried out in a 10 mL stainless-steel autoclave equipped with a Teflon liner. The standard reaction conditions involved 0.1 mmol of benzoic acid, 10 mg of Ru/HfB_2 catalyst (2.5 wt% Ru), and 1.0 mL of deionized water as the solvent. The reactor was pressurized with H_2 (4.0 MPa), heated to 80 °C, and stirred for 2 hours. After cooling and depressurization, the catalyst was separated by centrifugation, the product mixtures were identified and quantified by a SHIMADZU GC-2014C gas chromatography apparatus equipped with a SH-PolarWax chromatographic column and a flame ionizing detector. The main product is CCA, and the main by-product is 1-cyclohexene-1-carboxylic acid. The BA/Ru molar ratio is fixed at 20 assuming that the Ru is not leaching.

Hydrogenation of Proposed Intermediates

To experimentally validate the plausibility of the DFT-predicted hydrogenation pathway, isolated intermediate compounds were subjected to the same catalytic conditions as benzoic acid. Specifically, 2-cyclohexene carboxylic acid and 1,3-cyclohexadiene carboxylic acid were used as model intermediates representing partially hydrogenated species along the reaction coordinate. In a typical experiment, 0.1 mmol of the substrate was added to a 10 mL stainless-steel autoclave along with 10 mg of Ru/HfB_2 catalyst (2.5 wt% Ru) and 1.0 mL of deionized water. The reactor was sealed, purged three times with H_2, pressurized to 4.0 MPa H_2, and heated to 80 °C with stirring (600 rpm) for 1 hour. After cooling and depressurization, the reaction mixture was centrifuged to remove the catalyst, and the supernatant was analyzed by GC-FID and GC-MS. Both intermediates were found to undergo rapid and selective hydrogenation to cyclohexane carboxylic acid (CCA) with conversions exceeding 95% and product selectivities above 99%. These results confirm that the partially hydrogenated species are catalytically competent intermediates and support the proposed stepwise hydrogenation mechanism.

Hot Filtration Experiment

Reaction conditions: 0.1 mmol BA, 10 mg Ru/HfB_2, 1 mL H_2O, 80 °C, 4.0 MPa H_2, stirring at 600 rpm. At 60 min, the mixture reached ~52.4% conversion and was hot-filtered (preheated glass syringe and PTFE filter used to maintain ~80 °C). The filtrate (clear solution) was then sealed back in the reactor and reacted for another 60 min under identical conditions. Final BA conversion after total 2 h remained at ~52.6%, confirming no further reaction occurred in absence of catalyst

Kinetic Isotope Effect (KIE) Measurement

To evaluate whether the carboxylic proton in benzoic acid (BA) participates in the rate-determining step of the hydrogenation reaction, we performed a kinetic isotope effect (KIE) study by substituting the –COOH proton with deuterium (–COOD) to generate BA-d_1. In a typical run, 0.1 mmol of either BA or BA-d_1 was added to a 10 mL stainless steel autoclave along with 10 mg of Ru/HfB_2 catalyst and 1.0 mL of deionized H_2O. The reactor was sealed, purged with H_2 three times, then pressurized to 4.0 MPa and heated to 80 °C. After 2 h of stirring at 600 rpm, the reactor was cooled, depressurized, and the reaction mixture was filtered. The filtrate was analyzed using GC-FID and GC-MS.

Kinetic Reaction Order Determination

To investigate the reaction mechanism and determine the rate-limiting steps, reaction order studies were performed under differential conditions where substrate conversions were kept below 20%. All reactions were conducted in a 10 mL stainless-steel autoclave using Ru/HfB_2 catalyst (10 mg, 2.5 wt% Ru), with 1.0 mL of deionized water as solvent, at 80 °C and under magnetic stirring at 600 rpm. The reaction time was fixed at 15 minutes to ensure initial rate conditions.

For the determination of reaction order with respect to BA, the initial substrate concentration was varied from 0.05 to 0.30 mmol, while maintaining the hydrogen pressure at 4.0 MPa. For the hydrogen pressure dependence, BA concentration was fixed at 0.1 mmol, and H_2 pressure was varied from 1.0 to 4.0 MPa. After reaction, the mixture was cooled, filtered, and analyzed by GC-FID using n-decane as an internal standard. Initial rates were calculated based on CCA formation.

Log–log plots of initial rate versus substrate concentration or H_2 pressure were constructed (Figure S10). A linear fit of the data for BA concentration yielded a slope of 0.95, indicating a first-order dependence on BA. In contrast, a slope of 0.47 was obtained for hydrogen pressure, suggesting a half-order dependence on H_2. These findings indicate that BA adsorption or surface reaction is likely the rate-determining step, while hydrogen dissociation occurs via a pre-equilibrated process on the electron-rich $Ru^{\delta-}$ surface. This kinetic behavior aligns well with the proposed ring hydrogenation mechanism.

DFT Computational Details

Spin-polarized density functional theory (DFT) calculations were performed using the Vienna Ab initio Simulation Package (VASP). The Perdew–Burke–Ernzerhof (PBE) generalized gradient approximation (GGA) functional was used to describe electron exchange–correlation effects. The projector augmented-wave (PAW) method was employed to treat core–valence interactions, with a kinetic energy cutoff of 450 eV. The HfB_2 surfaces were cleaved from the optimized hexagonal bulk structure (space group: P6/mmm). Three different low-index surfaces—(100)—was modeled as slabs containing three atomic layers with a vacuum space of 15 Å in the z-direction. During geometry optimization, the bottom one or two atomic layers were fixed to simulate the bulk, while the top layers were fully relaxed. A (3 × 3) supercell was used to avoid lateral interaction between periodic images. To model the supported metal species, a Ru_{13} cluster (consisting of 13 Ru atoms in a trigonal bipyramidal configuration) was placed on the HfB_2 surface at various interfacial sites. The Ru cluster size was chosen based on HAADF-STEM observations of ~2 nm Ru nanoparticles, to approximate local geometric and electronic effects while maintaining reasonable computational cost. The Brillouin zone was sampled with a 2 × 2 × 1 Monkhorst-Pack k-point mesh, and the convergence criteria for electronic and ionic steps were set to 10^{-5} eV and 0.02 eV/Å, respectively. Charge density difference maps were generated to visualize electron transfer at the Ru–HfB_2 interface. Bader charge analysis was performed using the Henkelman group's algorithm to quantify the charge state of interfacial atoms. Additional side-view structural models of the full slab systems, including fixed/relaxed atom labels and Ru cluster configuration, are provided in Supplementary Figure S6.

Supplementary Table S1. Ru content of the evaluated catalysts based on the ICP-MS analysis.

Sample	Nominal loading (wt.%)	Results of ICP [a] (wt.%)
Ru/HfB_2	2.5	2.48
Ru/AC	2.5	2.47

[a] The selected Ru-based catalyst was added into aqua regia and boiled for 20 min. After cooling, the solution was filtered into a 25 ml capacity bottle and diluted with 5% hydrochloric acid solution. Samples were calcined in a muffle furnace with a heating rate of 4 °C min^{-1} at 550 °C for 4 h to burn off the carrier. The remaining Ru was dissolved in aqua regia and diluted with 5% hydrochloric acid in a 25 ml volumetric bottle.

Supplementary Table S2. Fitting parameters from the EXAFS spectra of the selected catalysts.

Sample	Scattering path	CN[a]	R (Å)[b]	$\sigma^2 \times 10^3$ (Å^2)[c]	R factor
Ru foil [1]	Ru-Ru	12	2.67±0.004	3.3±0.5	0.008
$RuCl_3$ [2]	Ru-Cl	4	2.33±0.01	5.2±2.5	0.007
Ru/HfB_2	Ru-Ru	6.1	2.68 ± 0.03	7.2±2.9	0.008
	Ru-B	4.3	1.82 ± 0.02	4.5 ±1.3	0.018
Ru/AC	Ru-Ru	12.2±1.3	2.67±0.05	3.5±1.8	0.009

[a] Coordination number. [b] Coordination shell distance. [c] Debye-Waller factor.

Supplementary Table S3. Catalytic performance of different catalysts.

Entry	Catalysts	t (h)	T (℃)	CCA yield (%)
1	HfB_2	2	80	2
2	Ru/AC	2	80	82
3	2.5% Ru/HfB_2	2	80	86
4	1.0% Ru/HfB_2	2	80	63
5	5.0% Ru/HfB_2	2	80	92

Reaction conditions: 0.1 mmol BA, 10 mg catalyst, 1 mL H_2O, 4 MPa H_2.

[a]TOF = calculated based on the total Ru loadings.

Supplementary Table S4. The results of the KIE experiments.

Substrates	**Conversion /%**	**Selectivity of CCA /%**	k_H **or** k_D **/min^{-1}**
BA (COOH)	86.1	99.99	0.0164
BA-d_1 (COOD)	85.7	99.99	0.0162

Supplementary Table S5. Hydrogenation of BA catalyzed by Ru/HfB_2 in different solvents.

Entry	Solvents	Conv. （%）	Sel. （%）
1	H_2O	99.71	99.99
2	E thanol	25.35	100
3	i-propanol	5.35	100
4	acetic acid	1.69	100
5	Dimethyl sulfoxide	0	0
6	N,N-dimethylformamide	0.21	100
7	dioxane	0.30	100
8	toluene	0.23	100

Reaction conditions: 12.2 mg BA, 10 mg catalyst, 1 mL H_2O, 80℃, 4.5 MPa H_2, 2 h

Supplementary Table S6. ICP-MS analysis of Ru leaching in filtrates after catalytic reaction.

Sample	**fresh Ru/HfB$_2$**	**used Ru/HfB$_2$**	**filtrate**
Ru (wt.%)	2.48	2.44	0

Supplementary Table S7. The adsorption energy of BA, H_2, CCA and intermediates.

Adsorption state	Adsorption Energy (kJ/mol)
BA/Ru/HfB_2(001)	-133.14
BA/Ru/HfB_2(100)	-345.42
BA/Ru/HfB_2(101)	-404.27
BA/AC	-298.14
H_2/Ru/HfB_2(001)	-65.42
H_2/Ru/HfB_2(100)	-57.31
H_2/Ru/HfB_2(101)	-67.64
H_2/AC	-56.73
CCA/Ru/HfB_2(001)	-98.41
CCA/Ru/HfB_2(100)	-135.08
CCA/Ru/HfB_2(101)	-258.58
CCA/AC	-6.25
C0	-404.27
C1	-567.33
C3	-477.60
C4	-458.30
C5	-544.18
C6	-338.66

Supplementary Table S8. The reactive experiments with isolated intermediates.

Substrate	**Conversion /%**	**Selectivity to CCA /%**
2-Cyclohexene carboxylic acid	97.2*	99.5
1,3-Cyclohexadiene carboxylic acid	95.8*	99.1
BA	86.1 (2h)	99.99

* Reaction conditions: Catalyst: Ru/HfB_2 (10 mg, 2.5 wt%); Substrate: 0.1 mmol; Solvent: H_2O (1.0 mL); Temperature: 80 °C; H_2 pressure: 4.0 MPa; Reaction time: 1 h.

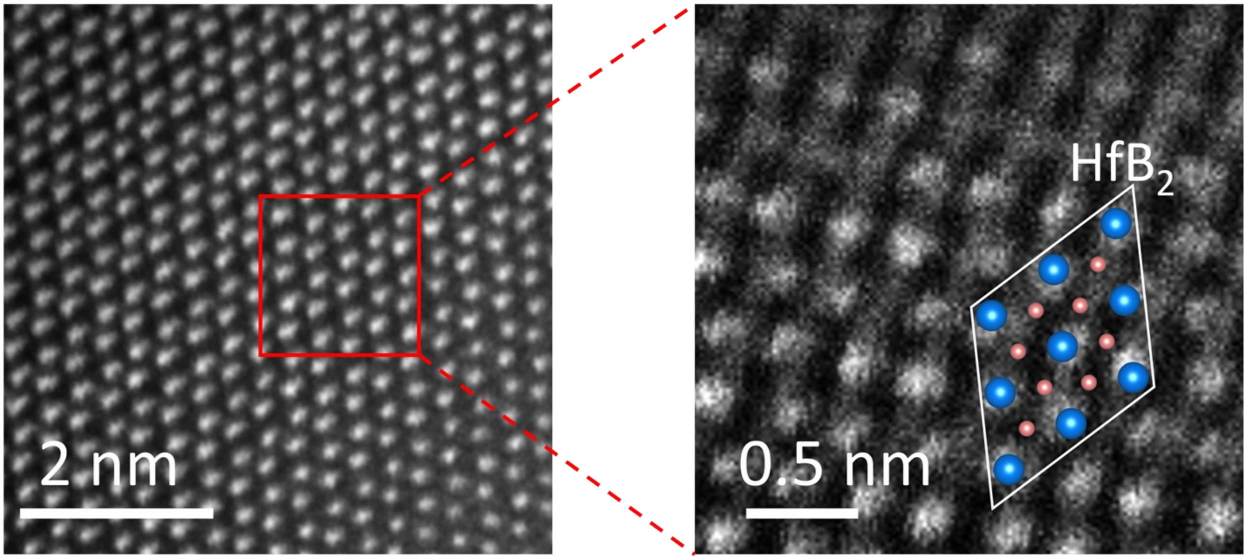

Supplementary Figure S1. High-resolution HAADF-STEM images of HfB_2 material.

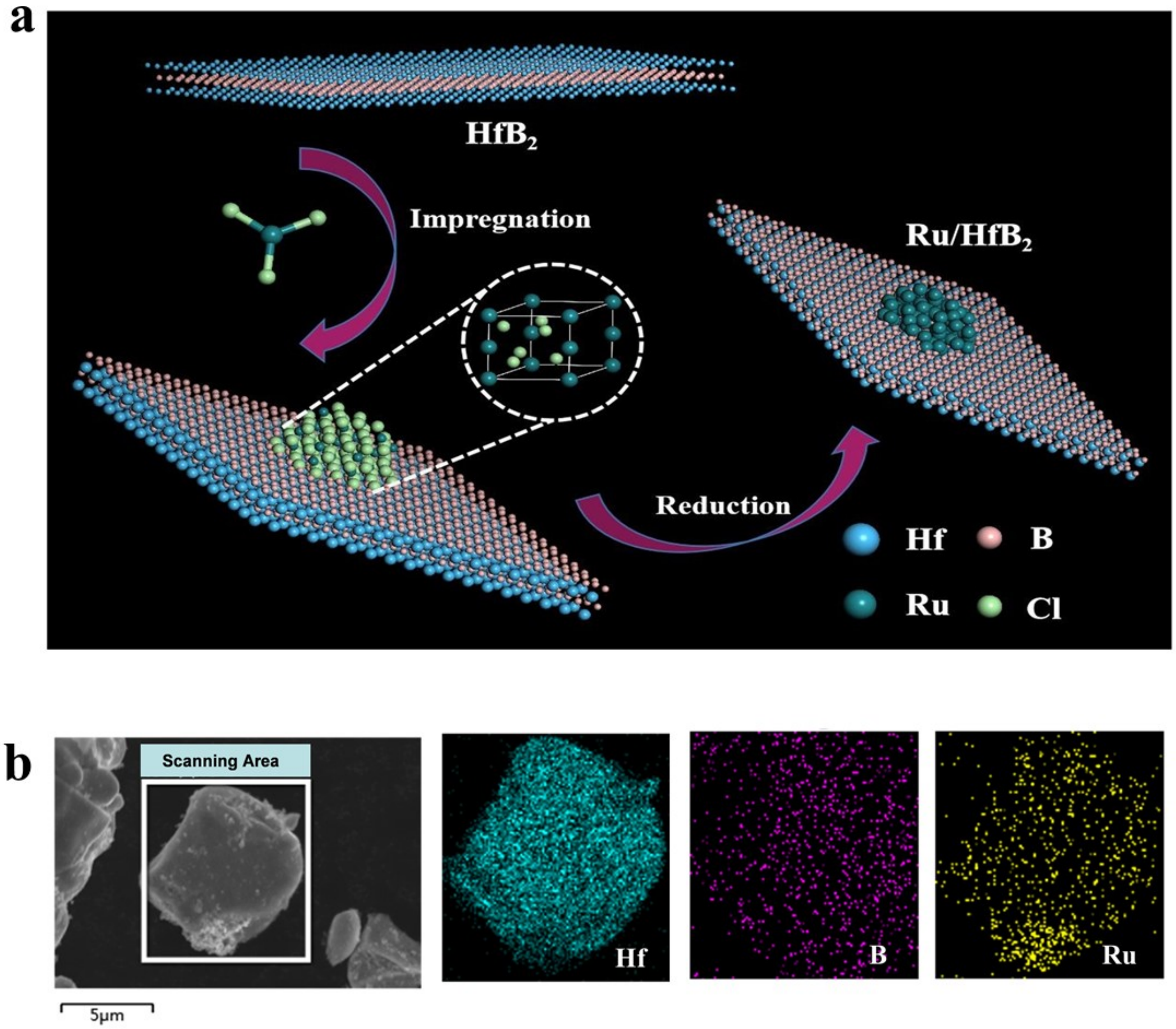

Supplementary Figure S2. (a) Schematic demonstration of the synthetic route for Ru/HfB_2 catalyst. (b) STEM element mapping images of fresh Ru/HfB_2 catalysts: Ru (yellow), B (purple), and Hf (blue), respectively.

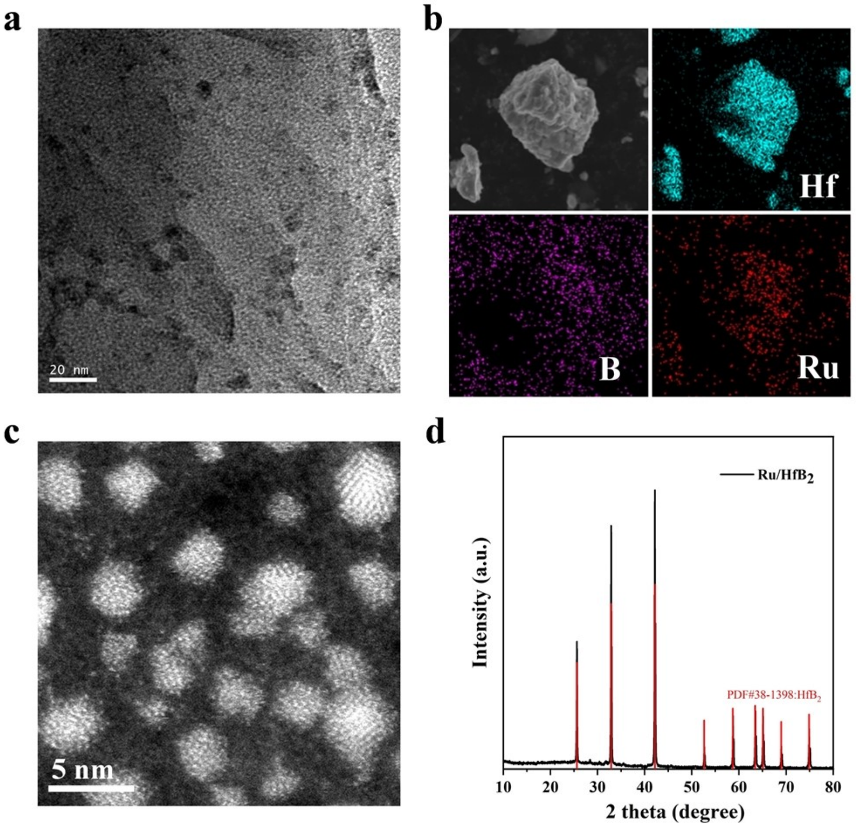

Supplementary Figure S3. Characterization of used Ru/HfB$_2$ catalysts. (a) STEM images of Ru/HfB$_2$. (b) STEM element mapping images of Ru/HfB$_2$: Ru (yellow), B (purple), and Hf (blue), respectively. (c) HADDF-STEM image of Ru/HfB$_2$ catalysts. (d) XRD patterns of Ru/HfB$_2$ catalysts.

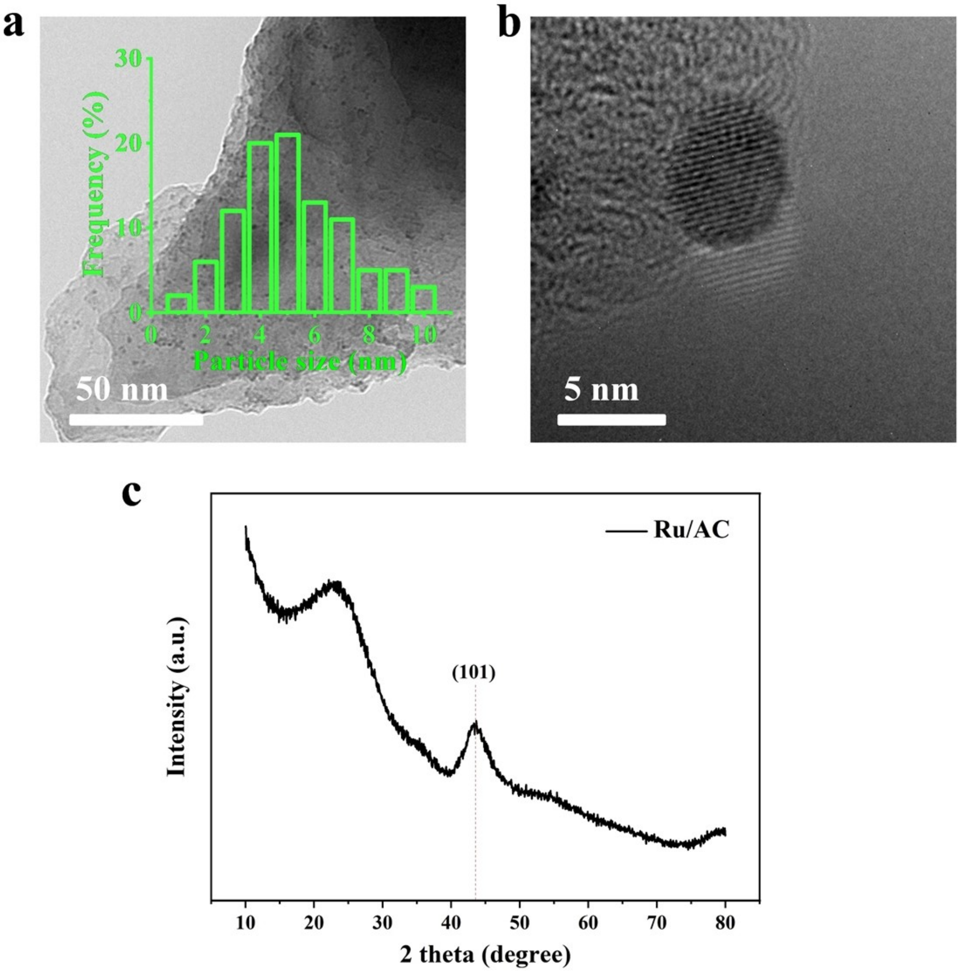

Supplementary Figure S4. Characterization of as-prepared Ru/AC catalysts. (a) STEM images of metal components in Ru/AC and particle size distribution histograms. (b) Representative HAADF-STEM images and (c) XRD patterns of Ru/AC catalysts.

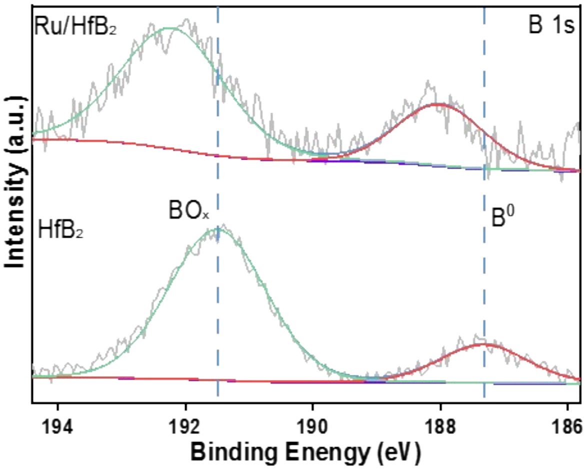

Supplementary Figure S5. B1s spectrum of Ru/HfB_2 and HfB_2.

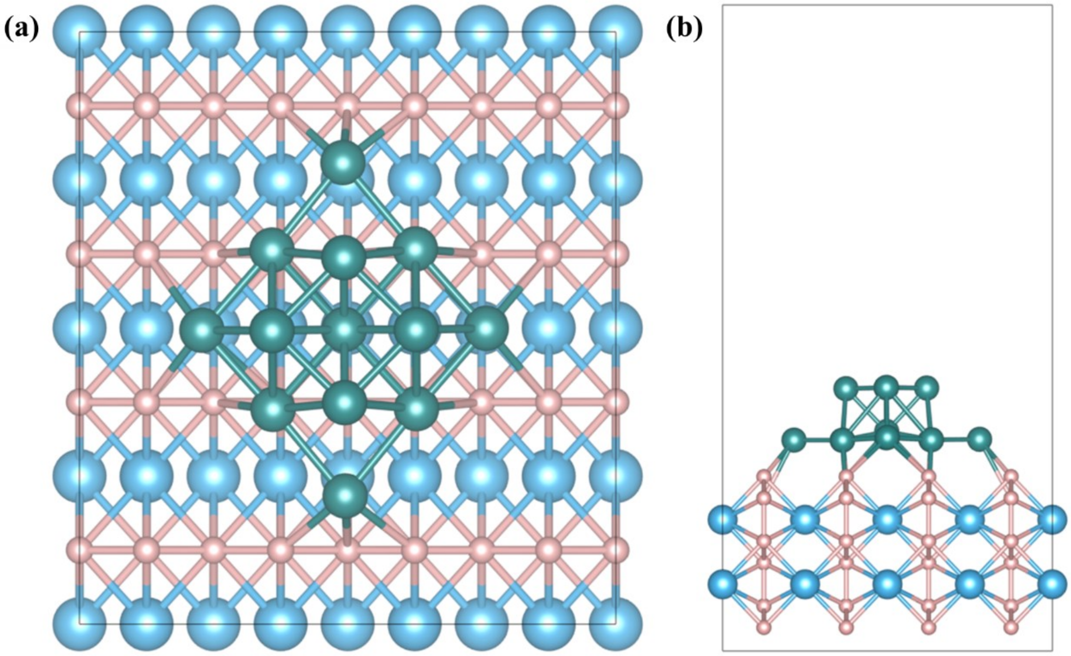

Supplementary Figure S6. DFT calculation model of Ru/HfB$_2$.(a) Top view and (b) side view.

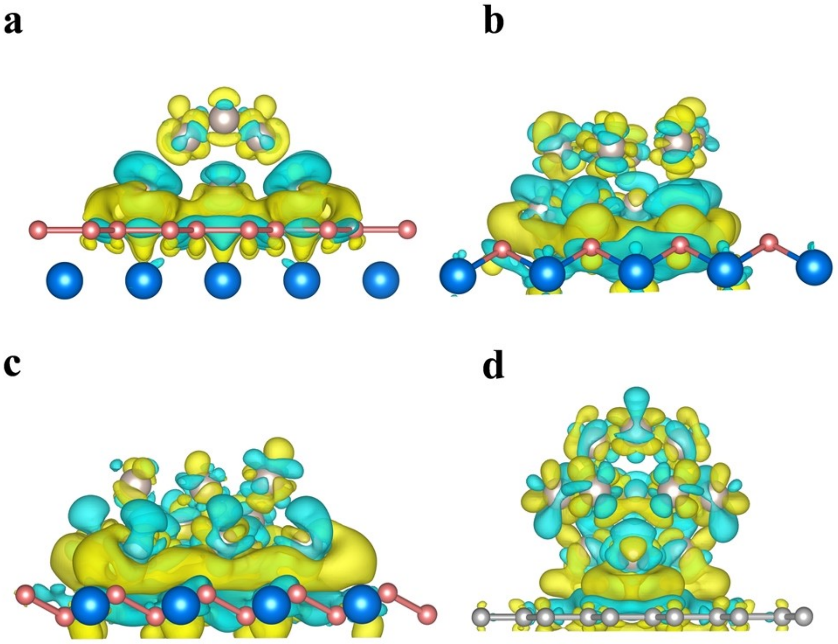

Supplementary Figure S7. Differential charge density of Ru/HfB$_2$. (a) Ru/HfB$_2$(001), (b) Ru/HfB$_2$(100), (c) Ru/HfB$_2$(101), (d) Ru/Graphene.

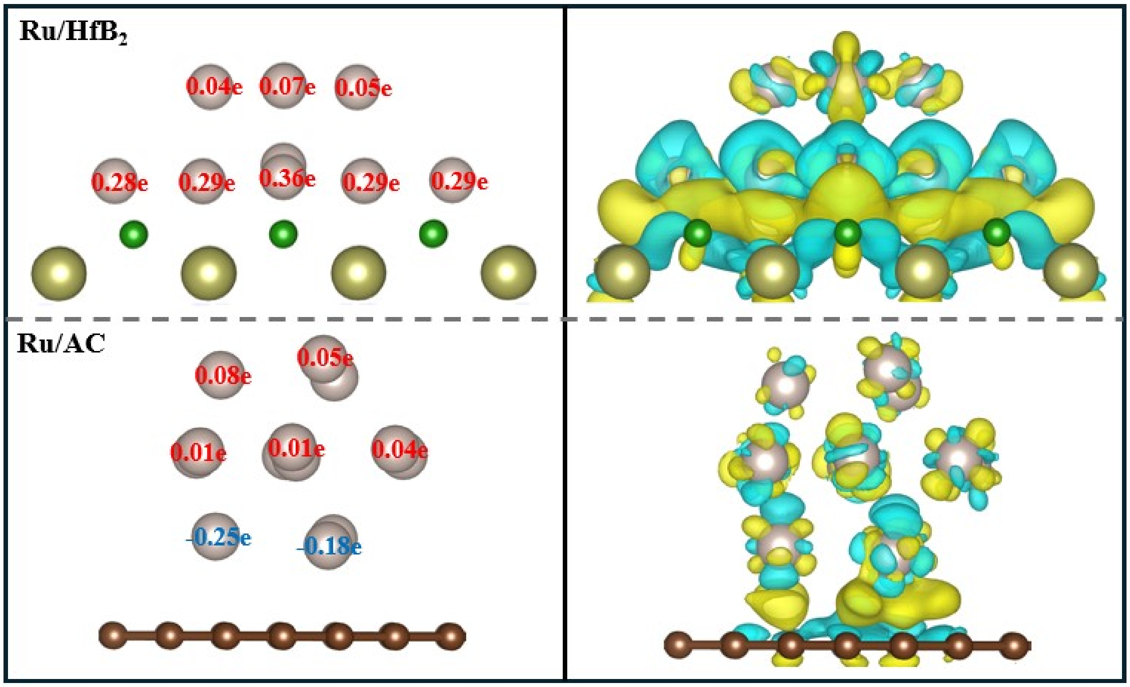

Supplementary Figure S8. Bader charge of Ru/HfB$_2$(100) and Ru/AC.

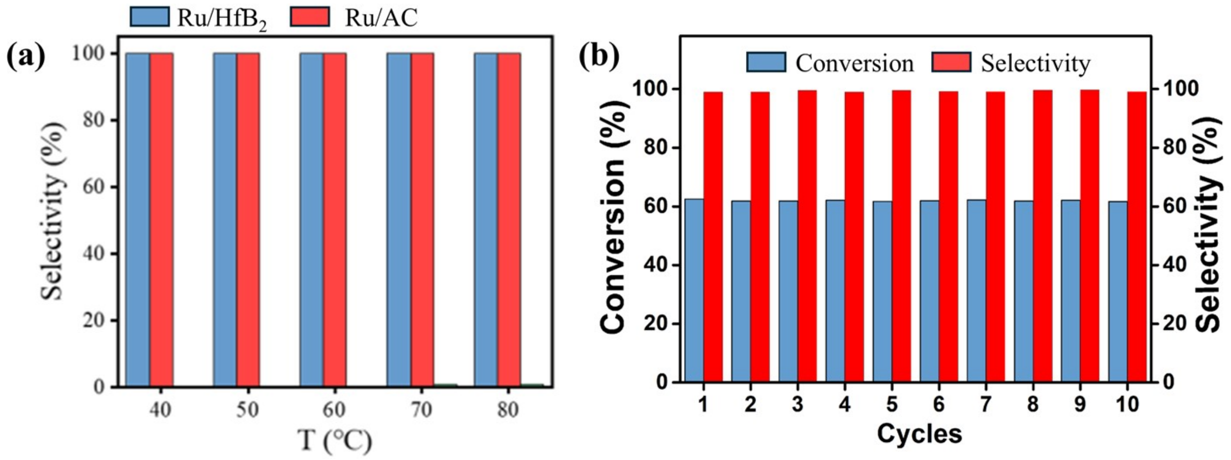

Supplementary Figure S9. (a) Effect of temperature on CCA selectivity. Reaction conditions: 0.1 mmol of BA, 10 mg catalyst, 1 mL H_2O, 4 MPa H_2, 2 h.; (b)Reuses of 2.5% Ru/HfB_2 for conversion and selective hydrogenation of BA. Reaction conditions: 24.4 mg BA, 20 mg catalyst, 2 mL H_2O, 80 °C, 4.5 MPa H_2, 2 h.

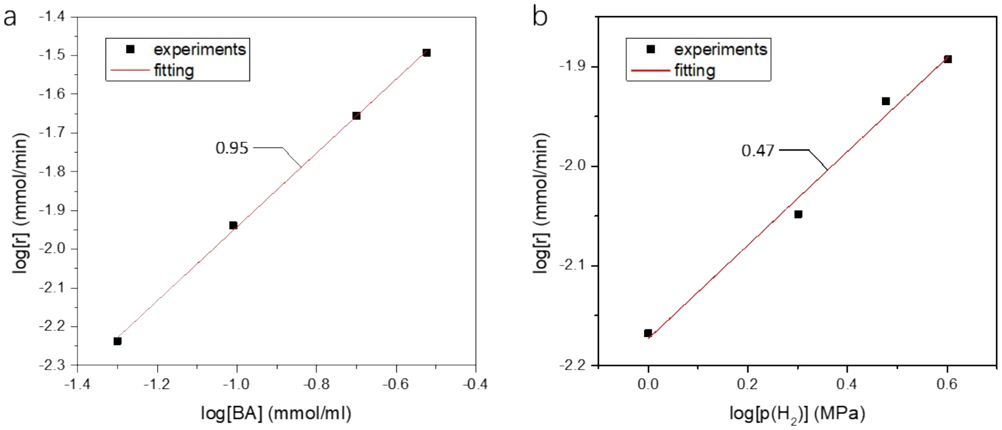

Supplementary Figure S10. Reaction rate, r, as a function of (a) the BA concentrations and (b) the partial pressure of H_2. The partial reaction order of both reactants is indicated by the slope (s) of the fitting lines. All kinetic studies were performed at a yield level of CCA <20%, where external and internal mass transfer limitations could be excluded. In order to circumvent the influence of catalyst deactivation, each point was obtained in a single experiment.

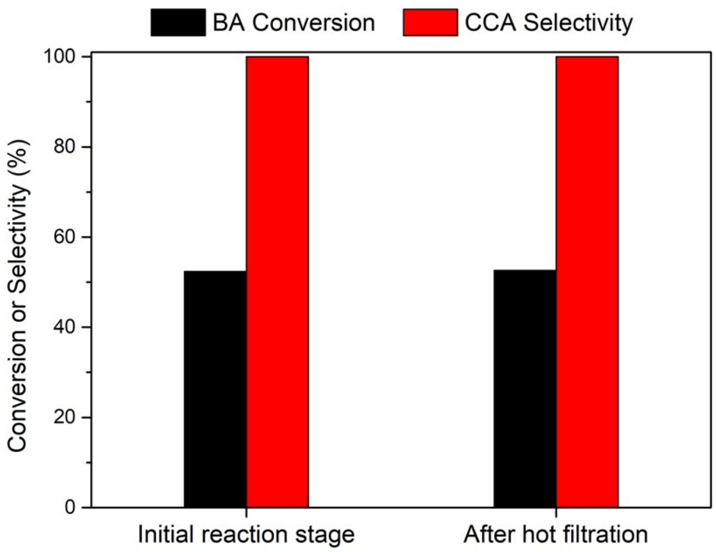

Supplementary Figure S11. Hot filtration test results (80 °C, 4.0 MPa H_2, 1 h).

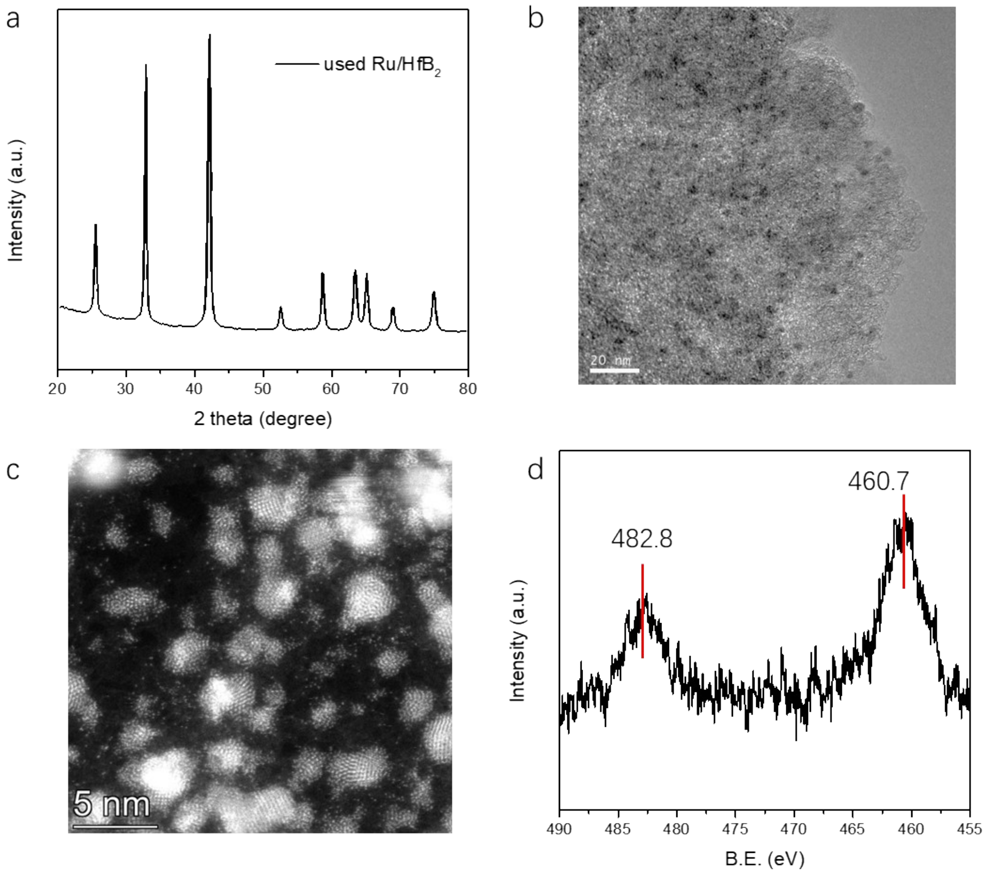

Supplementary Figure S12. Characterization of used Ru/HfB_2 catalyst. (a) XRD; (b) STEM, (c) HAADF-STEM and (d) Ru 3p XPS.

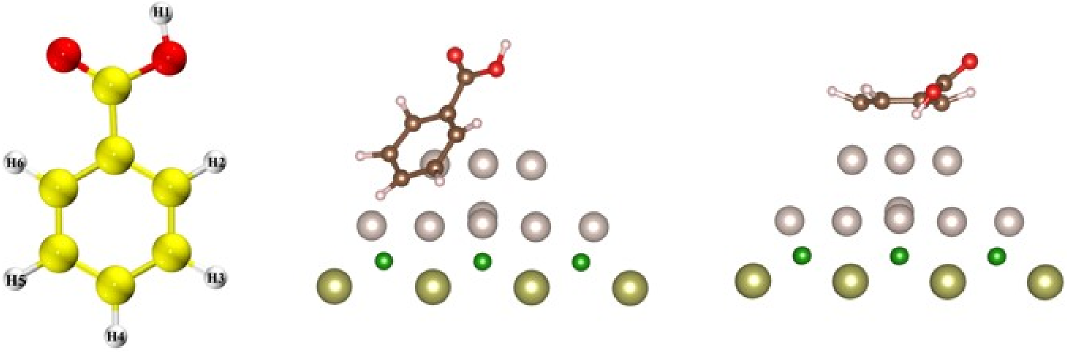

	H1	H2	H3	H4	H5	H6
BA	-0.64e	-0.11e	-0.06e	-0.10e	-0.09e	-0.12e
Side site	-0.70e	-0.11e	-0.15e	-0.13e	-0.11e	-0.10e
Top site	-0.67e	-0.12e	-0.09e	-0.12e	-0.17e	-0.16e

Supplementary Figure S13. The Bader charge adsorbed by BA on the side site and top site of Ru/HfB$_2$(100).